## Development of a Drag-Free Control System

Author: R. Haines

Principal Adviser: Dr. C. J. Eyles
School of Physics & Astronomy
University of Birmingham, UK

Email: rh@star.sr.bham.ac.uk

### ABSTRACT

A Drag-Free Control (DFC) system is a necessity for all future space-borne gravitational wave missions such as LISA, and similar technology is needed on other missions where high positional accuracy is required. The DFC system is needed to control the motion of the spacecraft that are required for the construction of a giant Michelson interferometer, which can be used to detect gravitational waves. Prior to this a technology demonstator mission is needed to test the feasibility of a drag-free spacecraft. This paper defines the requirements of the associated hardware (i.e. accelerometers, FEEP thrusters etc.) to be used in such a mission and details the control algorithms needed for the control computer such that a DFC system can be implemented and enable the required DFC performance of at least $\approx 10^{-13}$ ms$^{-2}$.Hz$^{-0.5}$ to be acheived.

## 1.     INTRODUCTION

The work described in this paper is part of on-going research to develop a drag-free control (DFC) system for future missions where high positional accuracy is required. Examples of such are gravitational wave missions like LISA and GAMMA and missions to test the Equivalence Principle such as STEP, MiniSTEP and Gravity Probe B. Similar technology will also be needed for other missions where high positional accuracy is required such as Darwin etc.

Gravitational waves are predicted by Einstein's General Theory of Relativity. They can be visualised as small-scale ripples in the curvature of space-time i.e. oscillatory distortions in the metric tensor $g_{nn}$ (which describes the curvature of space-time). Gravitational waves are thought to result from the acceleration of mass as predicted for compact astrophysical bodies such as binary stars, supernovae or massive black-holes in galactic nuclei. They are suggested to transmit the effects of the acceleration of masses with the speed of light $c$, in a similar manner to electromagnetic waves, which transmit the effects of the acceleration of charges, although gravitational waves are quadrupole in nature and electromagnetic waves are dipole.

To date no gravitational waves have been directly detected but detectors are being assembled on the ground and planned for space in order to try and detect them. There are two main frequency bands that will be observed in which possible gravitational wave sources may exist; these regimes are labelled high frequency and low frequency bands (10 Hz to several kHz and $10^{-4}$ Hz to 1 Hz respectively). The sensitivity of terrestrial detectors is limited due to the presence of random noises such as thermal, seismic, mechanical and gravity gradient noise (which are present on the ground), because the perturbations they would produce on a test mass would not be distinguishable from those generated by gravitational waves. The amplitude of seismic and gravity gradient noise becomes very large in the low frequency band and consequently terrestrial detectors are limited to the high frequency band above 1 Hz. However detectors in space are free from many of these noises and thus they are sensitive below 1 Hz and can therefore be used to observe in the low frequency band, where possibly more significant astrophysical sources can be observed.

The detection of gravitational waves will give another means of confirming general relativity and will provide a great deal of information about the astrophysical sources that generate them. Their detection could also hold the key to discovering new phenomena that have yet to be discovered, or even thought to exist. It has the possibility of opening up a whole new branch of astronomy, which is why several space missions have been proposed. The proposed space-borne missions will also compliment the work being carried out currently on the ground by terrestrial detectors, as

1

they are sensitive to the low frequency region, which is out of the domain of terrestrial detectors.

Passing gravitational waves cause a distortion in space-time, they act in the plane perpendicular to which they are travelling. If there were test masses present this distortion would result in the distances between the test masses changing i.e. they would expand and contract in anti-phase. An interferometer is an ideal instrument for accurately measuring these changes.

A drag-free control (DFC) system can be implemented using a free-floating proof mass enclosed within a spacecraft. This isolates the proof mass from the surrounding environment and thus its motion is not perturbed by any of the external surface forces (e.g. solar radiation pressure or atmospheric drag), but is only influenced by gravity. Consequently the proof mass will follow a geodesic, this behaviour is regarded as being drag-free. A DFC system aims to stabilise the spacecraft by operating its thrusters in such a manner that the thrust generated counteracts the external disturbances acting on the spacecraft. Thus the

spacecraft will follow the geodesic of the free-floating proof masses. The drag-free system consists of accelerometers, thrusters and a drag-free control computer which integrates all the subsystems together. The drag-free system does not make the spacecraft completely drag-free but just stabilizes it to a specified tolerance over a finite frequency range, thus enabling the signals of interest to be measured.

Future space-borne gravitational wave missions such as LISA[1] aim to detect gravitational waves by using a configuration of spacecraft (in which proof masses are housed) to form giant Michelson interferometers. The interferometer consists of an arrangement of spacecraft (e.g. three spacecraft in the case of LISA) that form the base of an equilateral triangle. One spacecraft is positioned at each vertex, thus creating an interferometer with armlengths[1] of $\approx 5 \times 10^6$ Km. Figure 1 shows a schematic of this configuration.
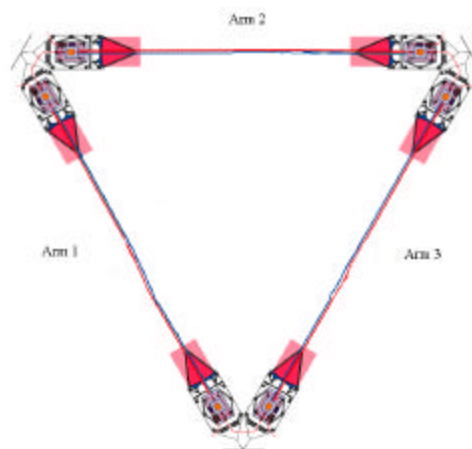


**Figure 1 : Schematic of the Layout for the LISA Interferometer**

The size of the arms created are defined by the seperation distance between the front faces of the proof masses that make up the sides of the triangular configuration. Each pair of arms acts like a one-bounce Michelson interferometer, i.e. the lasers are locked on to the front faces of the various proof masses (the proof mass faces act as the mirrors in a conventional interferometer) and laser beams are sent back and forth the interferometer arms and their phases monitored such that any changes in the distance between the

proof masses can be measured. However there are some differences in the arrangement compared with a conventional interferometer.[2] Each spacecraft has two optical benches which can act as the laser/beamsplitter/detector portions of a conventional interferometer and the other spacecraft proof masses in the arrangement act as the mirrors. Figure 2 shows a schematic of an optical bench.
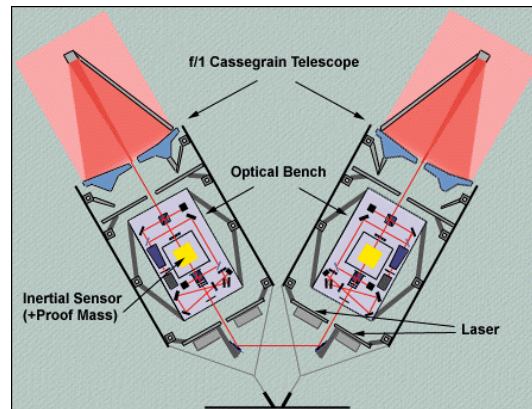
**Figure 2 : Schematic of Optical Bench**

Instead of having a separate beam splitter, each of the spacecrafts have two independent lasers that are phase locked and emitted along adjacent arms. When all instruments are functioning fully the configuration of spacecraft effectively form two independent Michelson interferometers which provides redundancy. This results because the optical benches on each of the spacecraft are identical and therefore enable the spacecraft to act as either the central beam splitter or as one of the end mirrors.

Due to the length of the interferometer arms the emitted beams power drops off greatly during its propagation which affects the overall sensitivity. Consequently to overcome this problem the original beam is not reflected back to the originating spacecraft but the spacecraft at the receiving end phase locks its local laser to the weak incoming signal and this higher power signal is then sent back to the originating spacecraft. The change in path length $\boldsymbol{DL}$ that would result from a passing gravitational wave is related to the amplitude of the gravitational wave (strain) $h$, by

$$h = \boldsymbol{DL}/L_o,\qquad\qquad(1)$$

where $L_o$ is the unperturbed path length. The phase difference measured by interferometric detectors can be increased by increasing their armlengths although this limits the maximum detectable frequency, consequently since LISA aims to have intereferometer armlengths of $\approx 5 \times 10^6$ Km it should be sensitive enough to be able to detect gravitational strains down to the level of $h \leq 10^{-23}$, which corresponds to a change in path length of $\approx 5 \times 10^{-14}$ m, in a one year observation with a signal-to -noise ratio of 5.[3] Using pairs of instruments within the spacecraft allows for redundancy of components, increases the probability

of detection and will enable the polarization of the gravitational waves to be determined.

The implementation of a DFC system is essential for spacecraft used in missions like LISA, since the spacecraft will be continually experiencing forces and torques (due external disturbances such as solar radiation pressure and atmospheric drag) which result in it constantly being perturbed during its passage through its orbit. These disturbances will induce errors into the determination of the interferometric path lengths and generate a noise which will drown out the signal due to the presence of possible gravitational waves. Thus a DFC system is needed to counteract these disturbances such that the spacecraft can be stabilised and the above effects eliminated, therefore enabling signals from passing gravitational waves to be measured.

Prior to the launch of space-borne gravitational wave missions a technology demonstrator mission such as the proposed ODIE[4] mission is needed. The objective of such a mission is to demonstrate the application of a drag-free control system to one spacecraft in order to achieve a new level of drag-free performance (i.e. the square root of the power spectrum of acceleration). This will be measured by a second accelerometer. In the ODIE proposal the aim is to control the position[4] of the spacecraft relative to its accelerometer proof mass to $x_{rel} \approx 10^{-9}$ m, this corresponds to a residual acceleration of $\approx 10^{-13}$ m.Hz$^{-0.5}$, which is a substantial improvement over the current drag-free performance record; the U.S Navy's TRIAD DISturbance COmpensation System (DISCOS)[5] obtained a residual

3

acceleration of $5\times10^{-11}$ ms$^{-2}$. In doing this, ODIE will also test the feasibility of its components such as the FEEP thrusters and high accuracy accelerometers and it will also provide knowledge regarding the known disturbances that will act on the spacecraft (e.g. solar radiation pressure, gradients in the magnetic fields and atmospheric drag).

This paper focusses on the determination of the control gains needed to provide the desired response of the spacecraft (i.e. control of the residual displacement of the spacecraft and proof mass to within $10^{-9}$ m for a selection of varying hardware requirements; namely how different sensor and actuator noises ($x_n$ and $feep_n$ respectively) affect the overall drag-free performance achievable and consequently what requirements are needed to achieve the drag-free performance of $10^{-15}$ ms$^{-2}$.Hz$^{-0.5}$ for future gravitational wave missions.

## 2. DRAG-FREE CONTROL SYSTEM

The drag-free system consists of accelerometers, thrusters and a drag-free control computer. An accelerometer[6] consists of a free-floating proof mass which is enclosed within a Ultra Low Expansion glass (ULE) chamber. The accelerometers are used to sense the motion of the proof mass relative to the spacecraft and to read out the drag-free performance this is achieved by measuring the position of the proof mass via capacitive sensing. The thrusters are micro-electric FEEP[7] (Field Emission Electric Propulsion) thrusters and are used to provide forces and torques to enable the spacecraft to maintain its position relative to the proof mass, so that the proof mass remains unaccelerated, except by space-time curvature and follows a geodesic. A secondary effect of the spacecraft following the path of the proof mass is that it too will behave in a drag-free manner although to a lesser degree of accuracy, however this is not a requirement but is desirable. The FEEP thrusters operational thrust range is expected to be between 4 and 30 µN. The DFC computer will be used to integrate all of the subsystems together, interpret the attitude and positional data from the accelerometers and determine the commands for optimum operation of the thrusters.

## 2.1 EXTERNAL AND INTERNAL DISTURBANCES

Before the control law algorithms could be designed and the corresponding DFC performance assessed, the missions orbit needed to be determined and the corresponding environment (disturbance sources) modelled. The simulation environment modelled was for a Geostationary Transfer Orbit (GTO, low inclination $i = 7°$, high eccentricity $e = 0.716$, with a perigee altitude of $\approx 620$ Km, an apogee altitude of $\approx$ 35883 Km and an orbit period of 10.6 Hours).[4] This was chosen because it is one of the worst case scenarios that the spacecraft may encounter and because there are readily available launch opportunities into orbits like this which is appropriate for a technoogy demonstrator. Thus if a DFC system can be implemented to give the desired drag-free performance for this case, then it should be possible for the majority of cases that may be encountered (i.e. Geostationary orbit etc). The principal external disturbances that the ODIE spacecraft will experience throughout this orbit will be due to:

1. Solar Radiation Pressure
2. Solar Wind
3. Atmospheric Drag
4. Earth's Magnetic Field
5. Gravity Gradients

All of these external disturbances cause the spacecraft to continually experience forces and torques, which result in it constantly being perturbed during its passage around its orbit. The DFC system aims to counteract these external disturbances and control the spacecraft in all six degrees of freedom ($x$, $y$, $z$, $f$ $q$ $y$). If the spacecraft deviates from the null position (i.e. the point of zero offset from the central position of the spacecraft relative to the proof mass) it will cause a force to act on the proof mass which is due to couplings between the spacecraft and the proof mass (i.e. due to the accelerometer and gravity gradients etc.). Consequently the more sensitive the degree of control of the spacecraft, the more these effects can be minimized. However, there will still be residual acceleration noise acting on the proof mass due to internal disturbances that act directly on the proof mass, such as:

1. Patch Fields and Contact Potentials
2. Electrostatic Forces
3. Magnetic Forces
4. Thermal Noise
5. Cosmic rays
6. Thermal distortions

All of these internal disturbances act directly on the proof mass and contribute in some way to inducing noises in the sensor and actuator outputs and these in

4

turn have a direct effect on the acceleration noise of the proof mass.

## 2.2     SENSOR NOISE

The sensor noise can be split into two components; force noise $f_n$, due to internal disturbances associated with the accelerometer and its surroundings and displacement noise $x_n$, which is associated with the design and construction of the capacitive sensing system. The force noise consists of two components $f_{n1}$ and $f_{n2}$. Whenever a motion sensor is used, it always induces a stiffness coupling within the system, in this case the use of the accelerometer will result in a stiffness coupling between the proof mass and the spacecraft of

$$f_{n1} = -\boldsymbol{b}x' - kx , \qquad (2)$$

where $\boldsymbol{b} (\approx 4.51 \times 10^{-9}$ Kg.s$^{-1}$) is the sensor viscous damping, $k$ ($\approx 0.925 \times 10^{-6}$ Kg.s$^{-2}$) is the sensor stiffness and $x'$ and $x$ are the relative velocity and displacement of the proof mass and spacecraft. The second force noise component $f_{n2}$, results from a combination of various force noises that are generated from many internal influences that act directly on the proof mass such as patch fields and contact potentials, thermal noise, detector back-action noise and actuator noise etc., although for this study this was assumed to be negligible in comparison to the $f_{n1}$ component.

The sensor displacement noise $x_n$, is an error that is always present in the final output signal of the accelerometer. It is defined by the design of the accelerometer sensing system i.e. its value is determined by what electronic components are used, the configuration chosen and the geometry of the electrodes (e.g. any asymetries incurred during the electrodes manufacture etc.). $x_n$ can be approximated to the thermodynamic noise that is associated with the amplifiers used in the sensor design, since this has the greatest contribution. Currently the displacement noise of the sensor[6] is estimated to be $x_n \approx 10^{-12}$ m.Hz$^{-0.5}$. The displacement noise will be fedback into the system and therefore an error will arise in the commanded thrust. This in turn will result in the spacecraft being incorrectly accelerated when trying to null the acclerometer readout and cause the spacecraft to be continually offset from its null position. Consequently all of these noise contributions and characteristics need to be included in the feedback

design models to ensure simulations for the behaviour of the DFC system are as realistic as possible.

## 2.3     ACTUATOR NOISE

A conservative noise level of 1% of the thrusters maximum output (i.e.$\pm 0.3$ μN) was assumed for the FEEP thrusters intrinsic noise[8].

## 2.4     CROSS-COUPLINGS

Cross-couplings between the 6 degrees of freedom can occur if there are misalignments e.g. between the sensor measurement axes and the actuator axes, or between the bodies calculated and actual centre of mass. Cross-couplings can also arise if there are products of inertia, these can occur if the body is not perfectly symmetrical or if the actuator torque axes are not aligned perfectly with the spacecrafts principal moments of inertia of the spacecraft. The presence of cross-couplings within the system will obviously affect the overall design of the DFC system and prevent the various axes from being modelled and analysed individually. Consequently the such effects need to be incorporated into the simulation control-loops. This will enable the effects to be characterized such that contraints can be set regarding acceptable levels for misalignments etc. that will still ensure that the desired DFC performance is acheived. However this work is on-going and thus will not be presented here.

## 3.     DRAG-FREE REQUIREMENTS

In order for future space-borne gravitational missions like LISA to be sensitive enough to detect gravitational waves, the proof masses need to be kept drag-free i.e. be free from accelerations within the measurement bandwidth ($10^{-4}$ to $10^{-1}$ Hz) to within an acceleration budget[1] of

$$S_a^{1/2} \approx 10^{-15} [1 + f/(3 \times 10^{-3})]$$
$$[((1+10^{-4})/f)^{1/3}] \text{ ms}^{-2}.\text{Hz}^{-0.5} , \qquad (3)$$

where $f$ is the frequency. To minimize the effects the internal disturbances (spacecraft-proof mass coupling, electrostatic etc.) have on the acceleration noise, the relative motion of the spacecraft to the proof mass must be controlled translationally[1] to less than

$$\delta_{z,s/c} < 2.5 \times 10^{-9} \text{ m.Hz}^{-0.5} , \qquad (4)$$

5

at a frequency of 1 Hz along the translational axes (which corresponds to a relative acceleration of $\approx 10^{-13}$ ms$^{-2}$.Hz$^{-0.5}$. The relative rotational control requirements[1] are

$$\delta_{\theta,s/c} < 1.5 \times 10^{-7} \text{ rad.Hz}^{-0.5} . \qquad (5)$$

This will enable the drag-free performance requirement for the mission to be met and ensure that the sensitivity to gravitational waves is adequate to achieve the scientific objectives.

## 4. CONTROL DESIGN

In order to test the performance of the DFC system that is being developed for translational and attitude control of the proposed ODIE spacecraft a simulation tool needed to be designed. This simulator was developed within MATLAB, a software package that includes the *simulink* toolbox that is specifically designed for modelling, simulating and analyzing dynamic systems. The simulation control-loop consists of

(i)     a plant (spacecraft and proof mass) with transfer function $P(s)$,
(ii)    a sensor (accelerometer) with transfer function $S(s)$,
(iii)   a disturbance with transfer function $D(s)$,
(iv)    a controller with transfer function $C(s)$
(v)     and an actuator (FEEP thrusters) with transfer function $A(s)$.

The transfer functions assumed for these components represent their dynamic behaviour. The results included in this paper were obtained from simulating one of the translational axes, namely the *x*-axis. Figure 3 shows a schematic of the generic control-loop that was applied for the translational motion. This was used to simulate the response of the proposed ODIE spacecraft and its associated proof mass to expected disturbances.
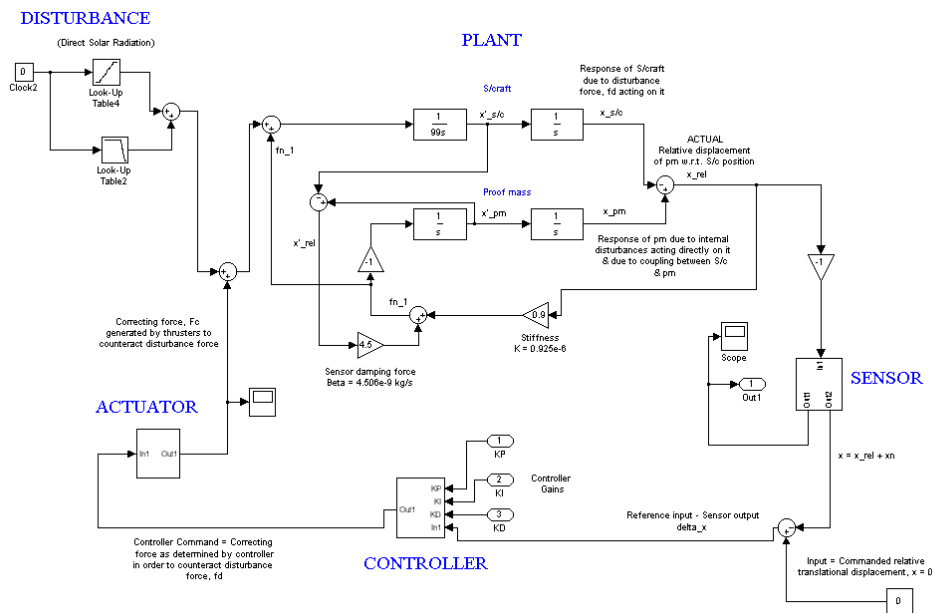


**Figure 3 : Schematic of Translational Control-Loop for One Axis**

The type of controller chosen was a PID (Proportional, Integral, Derivative) since their performance is robust for a wide range of operating conditions. A PID controller consists of the sum of proportional plus integral plus derivative control. The Laplace transform of a PID controllers output $U(s)$, is

$$U(s) = K_p + K_i/s + K_d/(1 + t(s)) , \qquad (6)$$

where $K_p$, $K_i$ and $K_d$ are the proportional, integral and derivative control gains respectively. This type of controller was chosen because it provides an acceptable degree of displacement error reduction simultaneously with acceptable stability and damping. For simplicity no couplings between the 6 degrees of freedom was assumed (the ideal case), so each control

6

R.Haines Author

loop could be investigated and modelled seperately.

The transfer functions determined for the dynamic behaviour of the spacecraft $(F(s)_{s/c})$ and proof mass $(F(s)_{pm})$ respectively in the translational x-axis were

$$F(s)_{s/c} = 1/(99s^2) , \qquad (7)$$

and

$$F(s)_{pm} = 1/s^2 , \qquad (8)$$

The spacecraft was proposed to have a mass budget of 100 Kg where the spacecraft's mass is 99 Kg and the proof mass is 1 Kg. The spacecraft is axially symmetrical, although the work reported here just considers independent axes.

### 4.1 OPTIMIZATION OF DRAG-FREE CONTROL GAINS

Simulations can only generate the response for a given system, they cannot indicate how the system can be modified i.e. what the form of the controller should be or what gains should be implemented to produce the desired response. The procedure of selecting the gains to give the optimum solution can be done either manually or automatically. Manual optimization can be achieved via intuition and many iterative refinements. Sets of empirical rules have been established regarding the tuning of PID controllers. Ziegler and Nichols have defined techniques that use results from either a closed-loop test (continuos cycling method) or an open-loop test (reaction curve method).[8, 9] Both methods objective is to produce a set of gains that result in a transient response with a decay ratio of 1/4. Alternatively automatic optimization of gain selection can be achieved via the application of optimization algorithms. Recently the application of Genetic Algorithms (GAs)[11] in control design and many other applications for optimization processes has been analysed and discussed by various authors.[12 - 15]

The use of a GA to optimize control gains has many advantages, the method performs a global search of the parameter space to find an optimum solution, its implementation is relatively straight forward and its operational speed is fast in comparison with manual approaches. A genetic algorithm is an optimization tool that is based on the concept of natural selection. The tool works by creating a random set of possible solutions that are used to produce new sets of solutions via "mutation" (i.e. the solutions parameters are altered) or via "sexual reproduction" (i.e. the parameters are either averaged or swapped between parent solutions). As this process progresses the weakest solutions (those that do not generate the desired control of the systems response) are supressed whilst the fitter solutions survive and are used for the creation of new and better solutions, in the same manner as natural selection.

Consequently the application of a GA to optimize the gains for the ODIE spacecraft drag-free controller was chosen. The requirements of the GA was to find the optimum gains such that the relative displacement of the spacecraft and proof mass is kept to a minimum, on average, throughout the orbit. In order to save some processing time the Ziegler-Nichols method[9-10] was initially used to define initial values and upper and lower boundaries for the PID controller gains. These could then be used as a starting point for the GA to work from.

### 4.2 PERFORMANCE OF CLOSED-LOOP

Due to time constraints the only disturbance that has been implemented in the closed loop simulations is the force due to direct solar radiation. The input disturbance was representative of the amplitude and time variance of the force generated by direct solar radiation around the Earth eclipse (as a worst case). The models were simulated for 1000 seconds as this provided sufficient time to represent realistic periods of variability in the disturbance force. Figure 4 shows a plot of the amplitude and time variation of the disturbance force used in the simulations. This ensured that the PID controller gains determined were optimum for keeping the relative displacement of the spacecraft and proof mass to a minimum overall, for all circumstances i.e. periods of maximum and minimum disturbance force. It was decided that this constraint would give meaningful results regarding what the DFC performance which could be achieved, since direct solar radiation is the principal disturbance that will be acting on the spacecraft for majority its orbit (although atmospheric drag is the greatest disturbance that the spacecraft will encounter, there is no requirement to sustain drag-free control around perigee because the resultant force is greater that can be generated by the FEEP thrusters and because it is only for a relatively short period of time). Consequently around perigee the spacecraft's attitude would be controlled by magnetorquers.
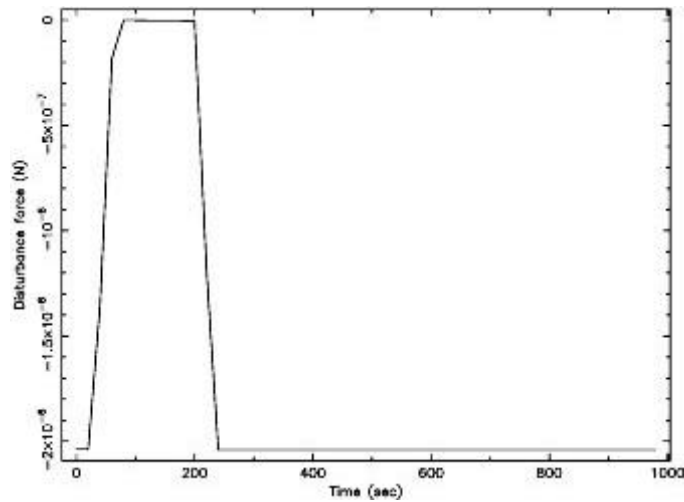
7

**Figure 4 : Plot of the Disturbance Force as a Function of Time**

The *x*-axis translational control-loop was simulated for a selection of different sensor and actuator noise levels to see how their magnitude affected the overall performance of the drag-free control system. Figure 5 shows a typical plot of the relative displacement of the spacecraft and proof mass as a function of time.

This can be used to calculate the power spectrum of the relative displacement as a function of frequency, which is shown in Figure 6.
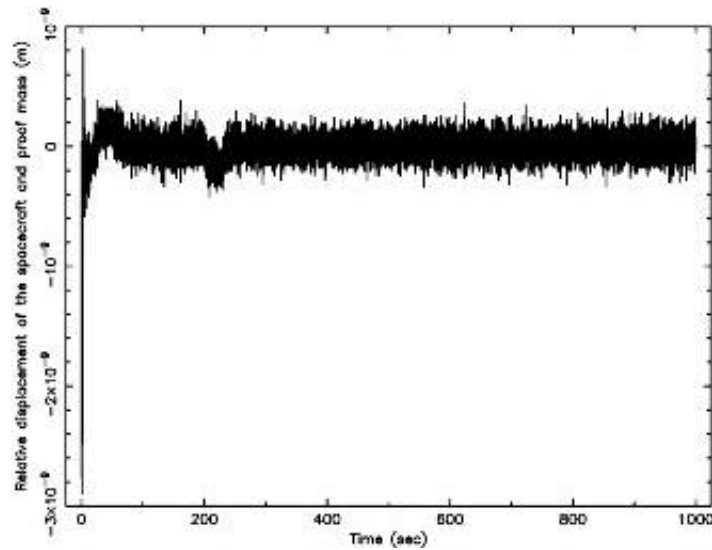


**Figure 5 : Plot of the Relative Displacement of the Spacecraft and Proof Mass as Function of Time**

8
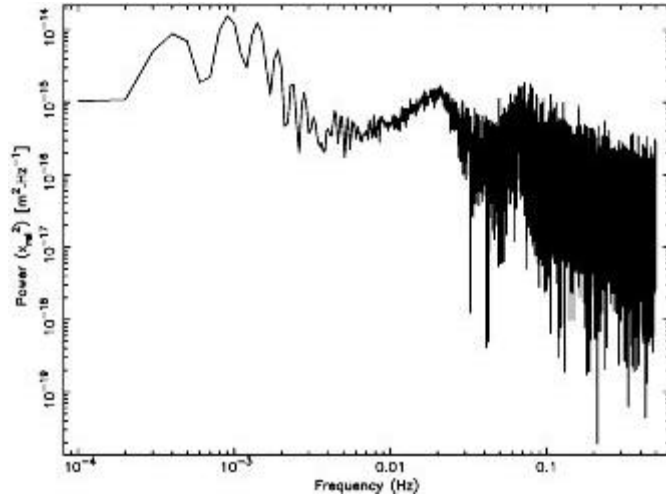
**Figure 6 : Power Spectrum of the Relative Displacement as a Function of Frequency**

For each combination of sensor and actuator noises cases simulated, the GA was used to determine the optimimum PID gains. After implementing these gains the total power spectra of the residual spacecraft displacements could be simulated and compared, the results are shown in Figures 7 and 8.
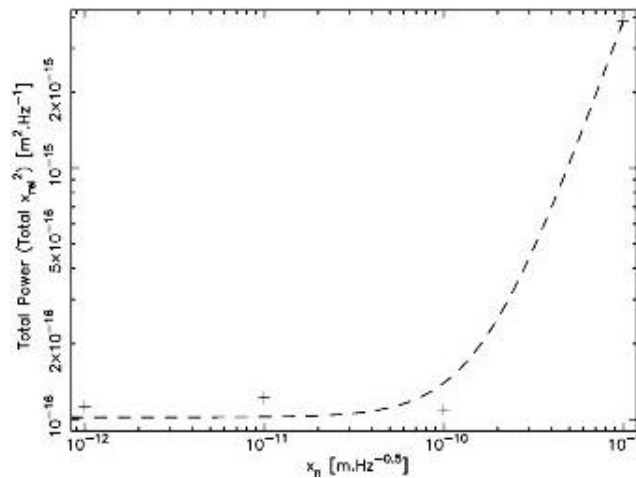


**Figure 7 : Total Power Spectra of the Relative Displacement as a Function of Sensor Displacement Noise**
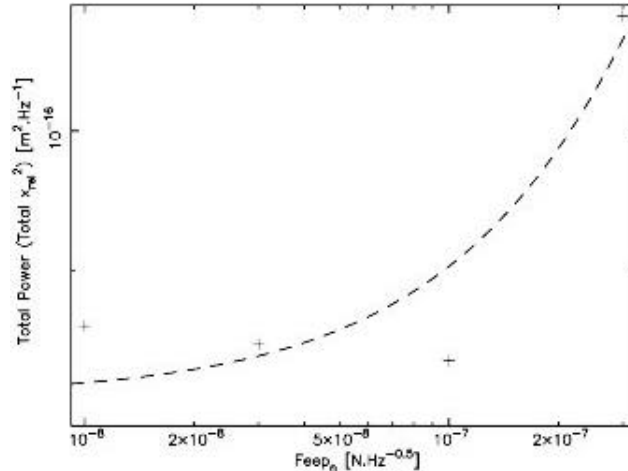
9

**Figure 8 : Total Power Spectra of the relative Displacement as a Function of Actuator Noise**

It can be seen from Figures 7 and 8 that there are limiting sensor ($x_n$), and actuator ($feep_n$), noise levels below which there is no significant gain regarding the reduction of the relative displacement ($x_{rel}$). The best DF performance was attained when the actuator noise was set to $feep_n \approx 1\times10^{-7}$ N.Hz$^{-0.5}$ and the sensor noise set to $x_n \approx 1\times10^{-10}$ m.Hz$^{-0.5}$, the corresponding acceleration noise achieved is shown in Figure 9. It can be seen that the DFC performance achieved at a frequency of 0.5 Hz is $\approx 2.3\times10^{-14}$ ms$^{-2}$.Hz$^{-0.5}$.
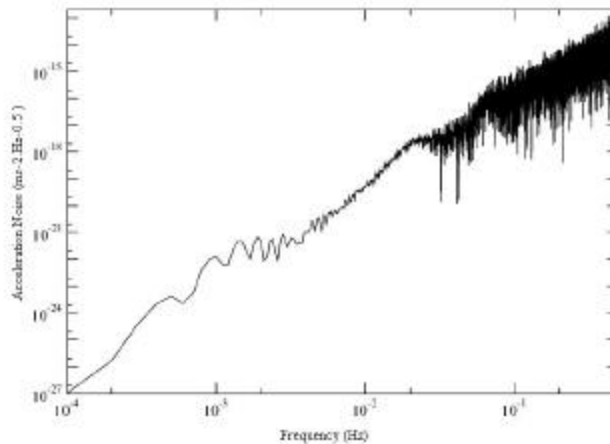


**Figure 9 : Plot of the Acceleration Noise as a Function of Frequency**

## 5.    CONCLUSIONS

The models developed above were based on reasonable assumptions regarding disturbance levels that may be encountered and noise levels that may be associated with the sensors and actuators. From analysis of their outputs it can be seen that the implementation of a DFC system enables the spacecrafts relative postion to be controlled to $\approx 10^{-9}$ m. We intend to carry out further investigations to characterize what the limiting sensor and actuator noises are for a given performance. The drag-free control requirements for future gravitational wave missions ($x''_{rel} \approx 10^{-15}$ ms$^{-2}$.Hz$^{-0.5}$)

can be met if the sensor and actuator noise levels are less than $x_n \approx 10^{-10}$ m.Hz$^{-0.5}$ and $feep_n \approx 10^{-7}$ N.Hz$^{-0.5}$ respectively. The results also indicate that the appication of a GA to determine the optimum gains required for the controller is an efficient and easy method to implement. However further analysis is required to determine if the drag-free control can be achieved for more complicated systems and situations e.g. systems that have cross-couplings between their axes and near perigee where atmospheric drag is the dominant disturbance. Investigations regarding the use of different control algorithms for different sections of the orbit would also be useful to determine if better

10

R.Haines Author

DFC performances can be attained throughout the orbit.

## 6.    ACKNOWLEDGEMENTS

## 7.    REFERENCES

[1]    Bender, P., et al, "Laser Interferometer Space Antenna for the Detection & Observation of Gravitational Waves, Pre-Phase A report.", 1998.

[2]    Young, H. D., "University Physics", Addison-Wesley Publishing, Reading, Massachussets, 1992.

[3]    Danzmann, K., "LISA & Ground-Based Detectors for Gravitational Waves: An Overview."In Proceedings of the 2nd International Symposium on the Detection & Observation of Gravitational Waves in Space, Pasadena, California, 1998.

[4]    Floyd, A., "Conceptual Design of an Orbiting Drag-free International Explorer (ODIE) Small Satellite Mission", Proceedings of the 11th AIAA/Utah State University Conference on Small Satellites, August 1997.

[5]    Staff of the Space Department, Johns Hopkins University Applied Physics Laboratory, Silver Spring, MD, & Staff of the Guidance & Control Laboratory, Stanford University, Stanford, CA. "A Satellite Freed of all but Gravitational Forces: TRIAD I", J. Spacecraft, vol. 11, No. 9, 1974.

[6]    Josselin, V., "Architecture mixte pour les accelerometres ultrasensibles edies aux missions spatiales de physique fodamentale", doctoral dissertation, University of South Paris, 1999.

[7]    Marcuccio, S., Genovese, A. & Andrenucci, M., "Experimental performance of FEEP microthrusters", Proceedings of the 3rd International Symposium on Space Propulsion, Beijing, China, 1997.

[8]    Saccoccia, G. and Berry, W., "European Development & Applications of Electric Propulsion Systems", Proceedings of the 50th International Astronautical Congress, Amsterdam, The Netherlands, October 1999.

[9]    Golten, J. and Verwer, A., "Control System Design & Simulation", McGraw-Hill Publishing, England, 1997.

[10]    Franklin, G. F. and Powell, J. D., "Feedback Control of Dynamic Systems",Addison-Wesley Publishing, Reading, Massachussets, 1986.

[11]    Holland, J. H., "Adaption in Natural & Artificial Systems", University of Michigan Press, Ann Arbor, 1975.

[12]    Lloyd-Davies, E., Ponman, T. J. and Cannon, D. B, "The Entropy & Energy of Intergalactic Gas in Galaxy Clusters", preprint, 2000.

[13]    Bennis, R. J. M., et al, "Feasibility Study of a Fuzzy Logic based Controller for Rendezvous & Docking of the Automated Transfer Vehicle (ATV) to the International Space Station (ISS)", Proceedings of the 50th International Astronautical Congress, Amsterdam, The Netherlands, October 1999.

[14]    Ortega, G., et al, "Geno-Fuzzy Control in autonomous servicing of a Space Station",Engineering applications of artificial inteligence, Elsevier, vol. 11, 1998.

[15]    Karr, C. L., et al, "Genetic Algorithm Based Fuzzy Control for Spacecraft Autonomous Rendezvous", Proceedings of the 5th Conference on Artificial Intelligence for Space Applications, May 1990.